

EVALUATION OF CRITICAL STRESSES FOR QUASI-BRITTLE MATERIALS AT VARIOUS LOADING RATES

Ivan Smirnov^{1*}, Alexander Konstantinov²

¹Saint Petersburg University, Universitetskaya nab. 7/9, St. Petersburg, 199034, Russia

²Research Institute for Mechanics, Lobachevsky State University of Nizhni Novgorod, Prospekt Gagarina 23, Nizhny Novgorod, 603950, Russia

*e-mail: i.v.smirnov@spbu.ru

Abstract. Engineering practice shows that the design of modern structures and technical components requires adapting existing methods for testing materials to dynamic load conditions. This work discusses the experimental and theoretical basis for determining and predicting critical stresses in quasi-brittle materials (such as concrete, rock, organic glass, etc.) over a wide range of loading rates provided by different test methods and equipment. Standard tests for compression, splitting and bending are presented. The incubation time approach is used as a unified approach for determining the dynamic strength of the materials. It is shown that critical stresses in the materials under a wide range of high-speed loads can be estimated based on two strength parameters.

Keywords: quasi-brittle materials, dynamic tests, strain rate dependence, dynamic strength, structural-temporal approach, incubation time

1. Introduction

Critical stresses in materials are dependent on load–time history. For example, ultimate strength, yield strength, and fracture toughness often depend on the rate and duration of loading/deformation [1-7]. With sufficiently slow loads, which are represented in standard tests, critical stresses usually vary within the limits of permissible errors and can be considered material constants. However, in the case of high-speed and shock loads, these constants do not correspond to real critical loads.

The dynamic strength of a material is usually estimated with a diagram of the dependence of the critical stress on a given strain rate. This empirical dependence can be approximated by a certain function [7-14], which can then be considered as a function characterising the strength behaviour of materials in a given range of loading parameters. However, this approach has several disadvantages. First, the stress/strain rate dependence of the critical stresses of a material should be available to engineers along with other common mechanical parameters. It remains unclear how these curves may be integrated into the reference parameter base of materials, and whether it is possible to estimate the dynamic strength of a material by analogy using the quasi-static approach. Second, the approximation curves remain unconnected to the physical essence of dynamic response of materials.

For example, the dynamic strength of rocks and concrete is often studied as a dependence of the critical failure stress on a strain rate [15-19]. These dependencies can be used for numerical simulation of specific engineering problems [20-22]. However, they are inconvenient for evaluating and comparing several materials or their internal conditions. It is

therefore necessary to offer parameters that will allow one to more simply evaluate and compare materials across a wide range of loading rates.

The structural-temporal approach [23] allows these drawbacks to be eliminated. This approach is based on the incubation time criterion [24], which implies that the critical value of a load pulse must be entered into a material for a certain time to initiate failure processes or structural changes in the elementary volume of the material. This specific time is the incubation time, which characterises the necessary duration of preparatory processes for failure or structural transformations of the material. In this case, the strength of a material under fast loads can be characterised by a constant with a dimension of time, rather than a set of critical stresses for given loading rates. In addition, this approach has a clear physical meaning, making it possible to explain the behaviour of the strain rate dependencies of critical stresses.

This paper considers the possibility of applying the concept of incubation time criterion to assess the critical stresses of brittle and quasi-brittle materials under high-speed loads in various loading schemes and installations. The aim of this work was to verify the applicability of this concept in the framework of one study in one laboratory, using the same materials and scale of samples, as well as loading installations and conditions for recording the controlled experimental parameters. Plexiglass and refractory brick ceramics were used as research materials. Compression, splitting and three-point bending of notched beams were performed. High-speed loads were carried out on an installation with a split Hopkinson pressure bar and a drop tower test machine.

2. Theoretical approach

Experimental results show significant variations in critical stresses depending on the shape, intensity and duration of the load. For example, in the case of sufficiently short impact loads, the material can withstand stress amplitudes many times greater than the critical stress at quasi-static loads [1,9]. With sufficiently slow loads, the critical stresses change within the limits of error. In this case, the failure condition at achieving a constant critical stress value works exhaustively. However, such a condition is not applicable to dynamic loads. In this case, the critical stresses are determined by the ratio of the duration of energy input into the elementary volume and the natural duration of structural changes within this volume.

The structural-temporal approach suggests considering a condition for an input of a structural force pulse for a period τ sufficient for failure of the elementary volume of a material [23,24]. For the case of brittle and quasi-brittle failure, this concept can be represented by the incubation time criterion [25]:

$$J \geq J_C \text{ or } \int_{t-\tau}^t \sigma(x, t') dt' \geq \sigma_C \tau, \quad (1)$$

where J is the local force pulse; J_C is the critical pulse; $\sigma(x, t')$ is the stress at a given point in the material; σ_C is the static ultimate strength; τ is the incubation time of failure or the dynamic strength. Thus, for failure at a given point in the material, it is necessary to accumulate a pulse value no less than $\sigma_C \tau$ within the incubation period. The parameters σ_C and τ are constants of a material, and τ is not depended on a load profile and duration.

The incubation time approach makes it possible to calculate the effects of unstable behaviour of critical stresses in materials observed in experiments under dynamic loading [24-26]. Condition (1) can be rewritten for the case of fracture initiation in the tip of an existing crack loaded by mode I [26]:

$$\int_{t-\tau_{ft}}^t K_I(t') dt' \geq K_{IC} \tau_{ft}. \quad (2)$$

Here, $K_I(t')$ is the stress intensity factor (SIF); K_{IC} is the critical SIF measured in quasi-static conditions; and τ_{ft} is the incubation time for crack initiation.

Failure of brittle and quasi-brittle materials under high-speed loads occurs at the growth stage of a load. Generally, this stage can be approximated by a linear function. Then, the integrands in (1) and (2) can be substantially simplified. This produces analytical expressions for critical stresses according to criteria (1) and (2).

For example, an increase in stress with strain can be assumed to be linear until it reaches the maximum value so that:

$$\sigma(t) = E\dot{\epsilon}tH(t) = \dot{\sigma}tH(t), \quad (3)$$

where $\dot{\sigma}$ is the stress rate; and $\dot{\epsilon}$ is the strain rate; and $H(t)$ is the Heaviside function. Substituting expression (3) into condition (1) when equality is fulfilled, one can find the time until the moment of macro-failure:

$$t^*(\dot{\epsilon}) = \begin{cases} 0.5\tau + \sigma_c/E\dot{\epsilon}, & t^* \geq \tau \\ \sqrt{2\sigma_c\tau/E\dot{\epsilon}}, & t^* < \tau \end{cases} \quad (4)$$

and combining (3) and (4) to obtain an expression for the coupling of critical stresses and the strain or stress rate:

$$\sigma^*(\dot{\epsilon}) = \begin{cases} \sigma_c + 0.5\tau E\dot{\epsilon}, & t^* \geq \tau \\ \sqrt{2\sigma_c\tau E\dot{\epsilon}}, & t^* < \tau \end{cases} \quad (5)$$

Expressions (4) and (5) can be used for the case of tension and compression, substituting the corresponding values of quasi-static ultimate stresses and the incubation times. For condition (3), the analytical expression can be obtained similarly using the load expression $f(t) = \dot{f}tH(t)$ in the SIF calculation.

3. Experimental methodology

Materials. Ceramic material (refractory clay brick) and organic glass (PMMA) were chosen as typical representatives of brittle and quasi-brittle materials.

The ceramic specimens were cut from the brick block. The cylindrical specimens for compression and splitting tests had a diameter of 18 mm and a height of 16 mm. The beams for bending tests had a length of 65 mm, a thickness of 10 mm, a width (height) of 15 mm and a notch of 2.5 mm. The notch tip was formed by the micro-indenter.

The cylindrical PMMA specimens for compression and splitting tests were cut from a rod with a diameter of 20 mm and height of 15 mm. The PMMA beams for bending tests were cut from a plate and had a length of 70 mm, a thickness of 10 mm, a width (height) of 15 mm and a notch of ~ 4 mm. The notch tip was formed using a razor blade.

Methods. The materials were tested using the compression and splitting of cylindrical specimens, as well as three-point bending of notched beams. The purpose of the experiments was to determine the critical stress leading to macro-failure/fracture, and the corresponding time for each loading rate. The measured loads and displacements made it possible to establish stresses in the cylindrical specimens and the SIF at the crack tip in the beams according to known formulas for mechanics of materials [27] and fracture mechanics [28].

In the presence of this experimental data, under conditions (1) or (2) there remains one unknown parameter - the incubation time. In this case, the incubation time can be estimated semi-empirically using the nonlinear approximation of calculated curves to experimental points via the damped least-squares method.

The tests under slow loads were carried out on a universal materials testing machine. The strain rate for compression and splitting was 0.1 1/s for PMMA and 0.001 1/s for ceramics. The beams were tested at a crosshead speed of 0.1 mm/min.

High-speed tests were carried out in two stages. The first stage consisted of tests on the installation using a split Hopkinson pressure bar (SHPB) [29]. The measuring bars were 20 mm in diameter. For bending tests, the span (distance between supports) was 50 mm. The stress and strain of the specimens were determined by the signals from strain gauges glued to

the measuring rods. A detailed description of the general measurement procedure and calculation formulas is well presented for compression and splitting in [30], and for three-point bending in [31]. It should be noted that the specimen sizes and pulse shape were selected to ensure an equilibrium state at both contacts of the 'specimen-bars', and to minimise inertial effects [32,33].

The second stage included tests using a drop tower test machine. A flat-tipped impactor with a diameter of 50 mm was used for compression and splitting tests, while a cone-tipped impactor was used in bending tests. The stresses in the specimens were determined by the signal from the piezoelectric sensor embedded in the impactor. The deformation of the specimens in these tests was not measured. When analysing the results of both installations, the loading rate was therefore substituted into formulas (4) and (5).

Therefore, the first stage of testing determined the stress rate dependencies of critical stresses in the materials. Next, the analytical curves were obtained on the basis of the experimental data of the first stage and expressions (4) and (5). The second stage of testing allowed for verification of the theoretical curves when using fundamentally different equipment and an alternative range of loading rates.

4. Results

Compression tests. The compression test results are presented in Fig. 1 and 2. The critical stress increases and the time to failure decreases with increased stress rate. The calculated curves obtained by Eq. (4) and (5) coincide well with the experimental points obtained during the SHPB setup. The parameters used in the calculations are given in Table 1.

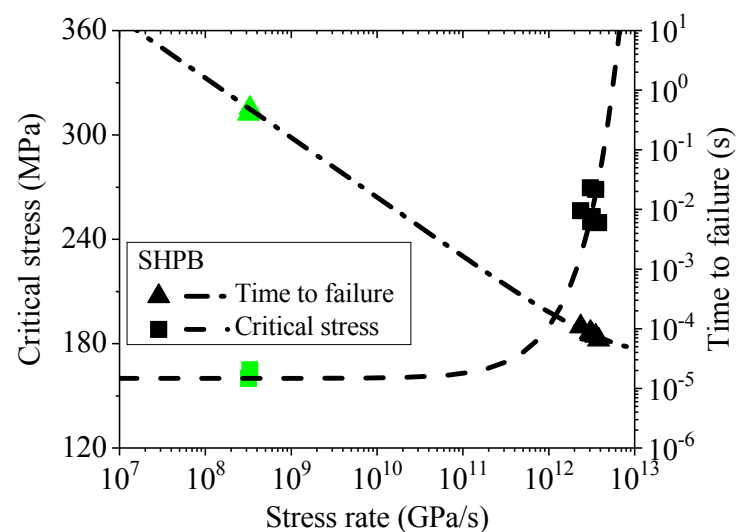


Fig. 1. Dependencies of the critical failure stress and the time until the onset of macro-failure on the strain rate for PMMA under uniaxial compression. Points are a result of the experiment; curves are calculations according to criterion (1)

Table 1. Strength parameters of the materials under compression

Material	σ_c [MPa]	τ_c [μ s]
PMMA	160	60
Refractory brick material	20.7	46

The results of the tests on a drop tower test machine are presented only for the ceramic material, since these loads were inadequate for the failure of PMMA. The experimental points from another range of stress rates catch significantly on the calculated curves, despite being obtained from a fundamentally different test setup. However, the results of tests carried out on

the DTTM installation have greater variation than the results of the SHPB installation. This is naturally due to the rougher implementation of experiments on a DTTM installation.

Therefore, the stress rate dependence of the critical stresses during compression tests can be calculated based on two parameters of a material.

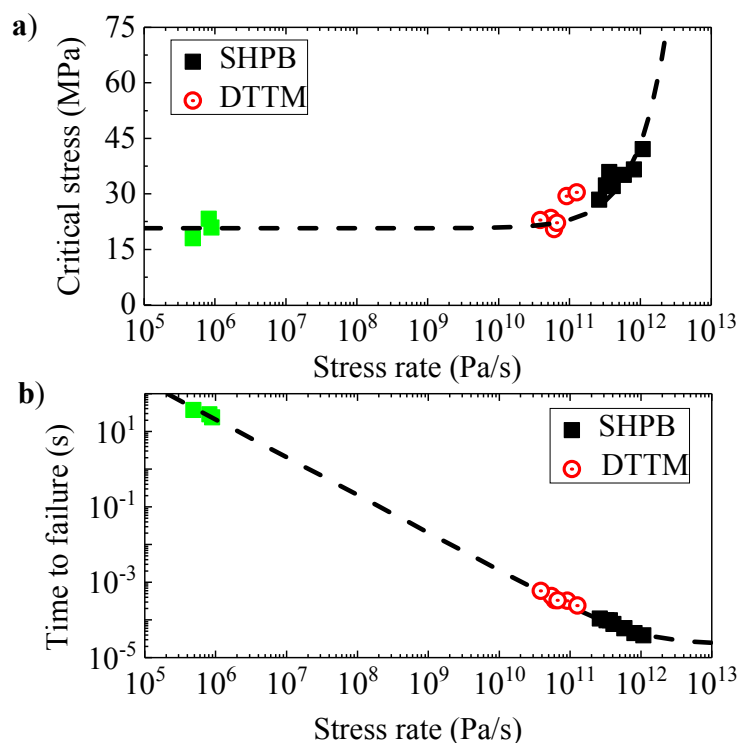


Fig. 2. Dependencies of the critical failure stress (a) and the time until the onset of macro-failure (b) on the strain rate for refractory brick material under uniaxial compression. Points are a result of the experiment; curves are calculations according to criterion (1). Green square points correspond to a slow load; black square points and red round puncture points correspond to high-speed tests on the SHPB installation and DTTM installation, respectively

Split cylinder tests. The splitting test results are presented in Fig. 3 and 4. Green square points correspond to a slow load, while black square points and red round punctured points correspond to high-speed tests on the SHPB and DTTM installations, respectively. The behaviour of the critical stress and time to splitting with increasing strain rate is comparable to the compression tests.

The stress rate dependencies of critical tensile stress and time before splitting were calculated by expressions (4) and (5) (see curves in Figs. 3 and 4). The calculation parameters are presented in Table 2. It is evident that the experimental points obtained at different installations have a different range of stress rates. However, both ranges are clearly described by a single curve, which was obtained using only two material parameters.

Table 2. Strength parameters of refractory brick ceramics during split tests

Material	σ_t [MPa]	τ_t [μ s]
PMMA	35	25
Refractory brick material	2.4	48

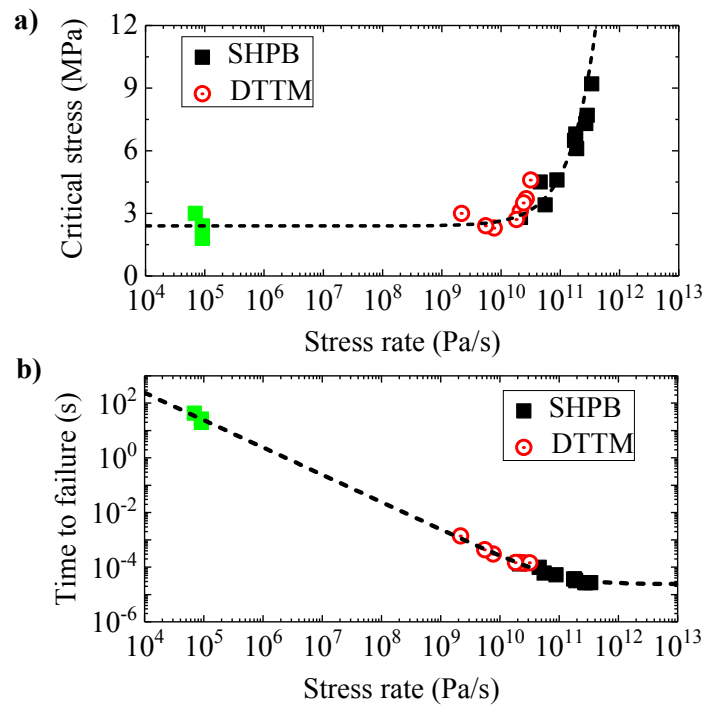


Fig. 3. Dependencies of the critical failure stress (a) and the time until the onset of fracture (b) on the strain rate for refractory brick material under splitting of cylindrical specimens

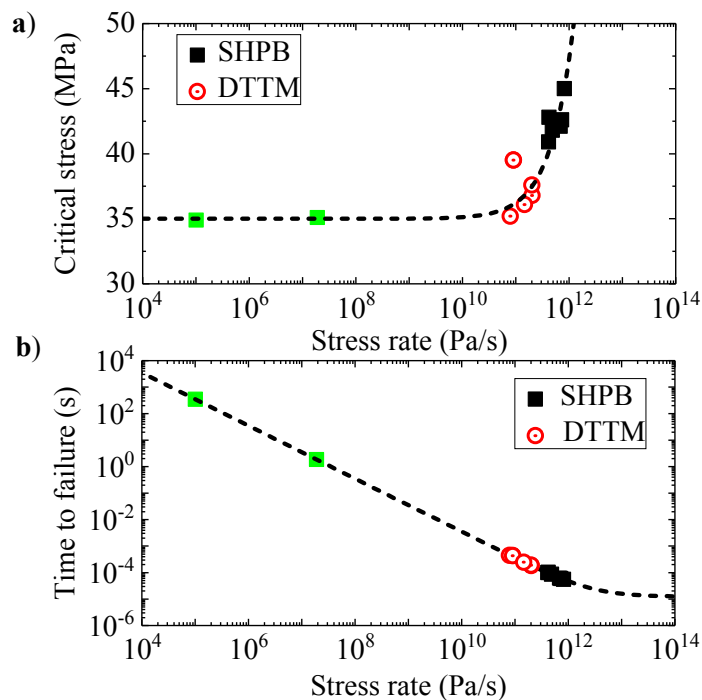


Fig. 4. Dependencies of the critical failure stress (a) and the time until the onset of macro-failure (b) on the strain rate for PMMA under splitting of cylindrical specimens

Fracture toughness tests. The dependence of fracture toughness and the time before fracture on loading rate are presented in Fig. 5 and 6. Green (square or triangular) points correspond to a slow load, while black (square or triangular) points and red round puncture points correspond to high-speed tests on the SHPB and DTTM installations, respectively.

Both experimental techniques provided a clear pattern of growth in the critical stress intensity factor with increasing loading rate.

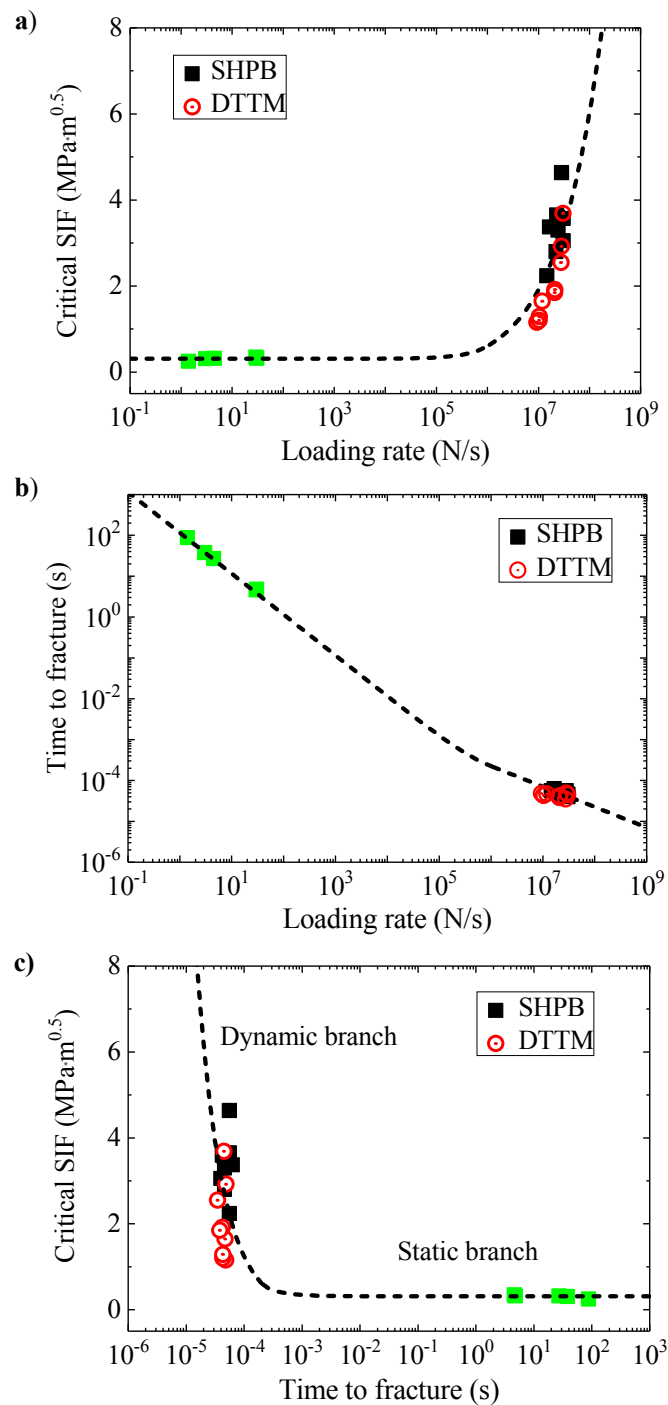


Fig. 5. Results for the refractory brick ceramic material subjected to bending tests. Curves correspond to calculations by criterion (2). a) Dependence of fracture toughness on loading rate; b) Dependence of time until the onset of crack propagation on loading rate; c) Time dependence of the critical stress intensity factor

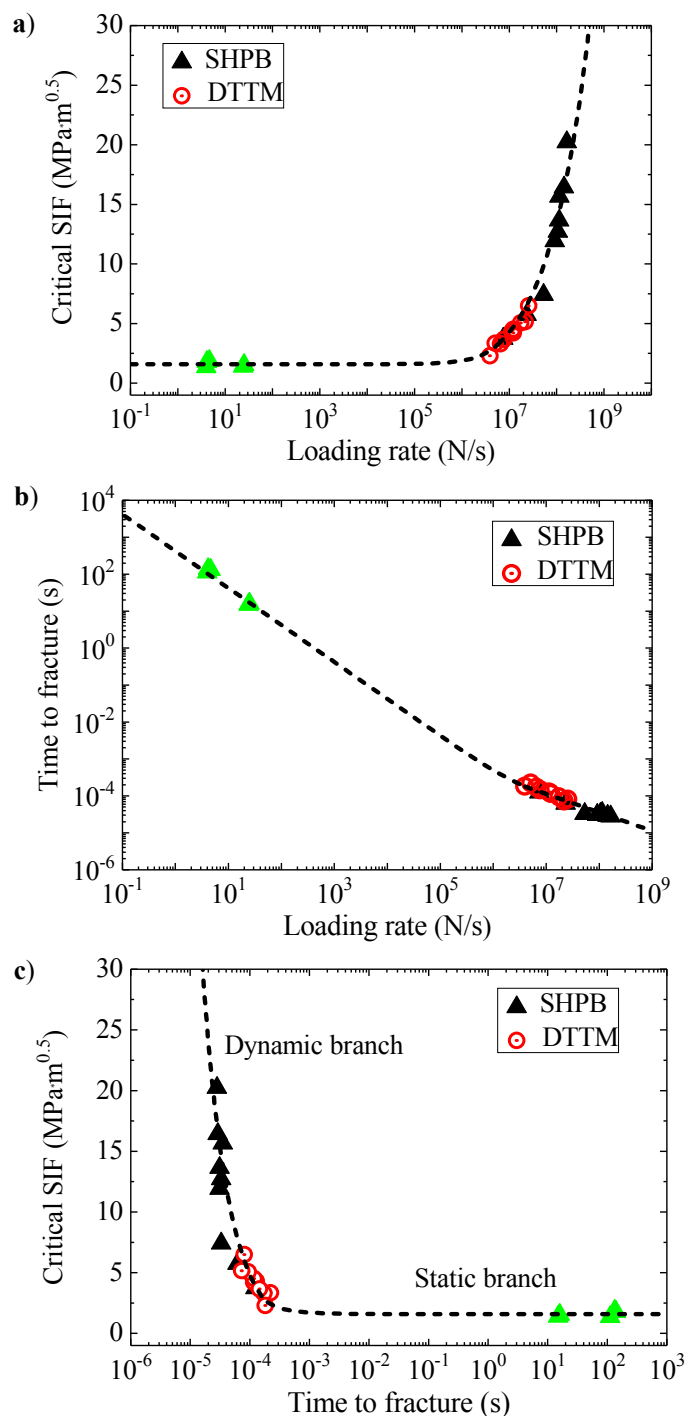


Fig. 6. Results for PMMA during bending tests. Curves correspond to calculations by criterion (2). a) Dependence of fracture toughness on loading rate; b) Dependence of time until the onset of crack propagation on loading rate; c) Time dependence of the critical stress intensity factor

At high loading rates, the critical SIF exceeds the values of the quasi-static critical SIF K_{IC} many times over. Therefore, based on a quasi-static approach, the procedure for estimating the crack resistance of materials under dynamic tests will provide correct data only for greater times before crack propagation.

The observed dependencies were calculated by criterion (2) by analogy with the case of compression or splitting. The corresponding parameters are presented in Table 3. The

calculated curves are in positive agreement with the experimental points. Thus, only two parameters are needed to predict fracture initiation for brittle and quasi-brittle materials under high-speed loading.

Note that the dependence of the critical stress intensity factor on the time to fracture manifests in two branches. One branch corresponds to the time to fracture $t \geq \tau$, when the influence of loading rate is negligibly small. This branch can be attributed to slow quasi-static loads. The second branch corresponds to the time to fracture $t \leq \tau$, when the critical SIF varies significantly. This branch responds to high-speed loads.

Table 3. Strength parameters of materials under three-point bending of notched beams

Material	K_{IC} [MPa \sqrt{m}]	τ_{ft} [μ s]
PMMA	1.6	152
Refractory brick material	0.31	220

5. Conclusions

The work aimed to study the possibility of evaluating critical stresses for quasi-brittle materials under slow and high-speed loads in various loading schemes and installations using the unified concept of incubation time criterion. Refractory brick ceramic material and organic glass were tested by the compression and splitting of cylindrical specimens, as well as three-point bending of notched beams. The studies were planned to first obtain experimental data on the stress rate dependence of critical stresses for one installation. This data was then used for analytical modelling based on the incubation time approach. The last stage included confirmation of the obtained calculation curves using a fundamentally different test method.

According to the obtained results, dependencies of critical compression or splitting stresses and critical stress intensity factors can be predicted based solely on the concept of incubation time criterion. In addition, this criterion makes it possible to predict the start time of macro-failure and crack propagation for a given loading rate.

The use of data with different ranges of loading rates obtained from different equipment and its positive agreement with the calculations suggests that the stress rate dependencies of critical stresses can be determined only by two material parameters. The first is a well-known quasi-static strength characteristic. The second is the incubation time, which is considered as dynamic strength in units of time.

Therefore, this approach can be used in the development of dynamic testing standards for brittle and quasi-brittle materials.

Acknowledgements. *The work was funded by the Russian Science Foundation (Grant № 18-79-00193).*

References

- [1] Meyers MA. *Dynamic Behavior of Materials*. USA: John Wiley & Sons, Inc.; 1994.
- [2] Ravi-Chandar K. *Dynamic fracture*. Elsevier; 2004.
- [3] Cadoni E, Forni D, Bonnet E, Dobrusky S. Experimental study on direct tensile behaviour of UHPFRC under high strain-rates. *Construction and Building Materials*. 2019;218: 667-680.
- [4] Pająk M, Janiszewski J, Kruszka L. Laboratory investigation on the influence of high compressive strain rates on the hybrid fibre reinforced self-compacting concrete. *Construction and Building Materials*. 2019;227: 116687.
- [5] Prakash G, Singh NK, Sharma P, Gupta NK. Tensile, compressive, and flexural behaviors of A15052-H32 in a wide range of strain rates and temperatures. *Journal of Materials in Civil Engineering*. 2020;32(5): 04020090.

- [6] Madivala M, Bleck W. Strain rate dependent mechanical properties of TWIP steel. *JOM*. 2019;71: 1291-1302.
- [7] Yang L, Lin X, Gravina RJ. Evaluation of dynamic increase factor models for steel fibre reinforced concrete. *Construction and Building Materials*. 2018;190: 632-644.
- [8] Chen X, Wu S, Zhou J. Experimental study on dynamic tensile strength of cement mortar using split Hopkinson pressure bar technique. *Journal of Materials in Civil Engineering*. 2014;26(6): 04014005.
- [9] Antoun T, Seaman L, Curran DR, Kanel GI, Razorenov SV, Utkin AV. *Spall Fracture*. New York: Springer; 2003.
- [10] Hao Y, Hao H. Numerical investigation of the dynamic compressive behaviour of rock materials at high strain rate. *Rock Mechanics and Rock Engineering*. 2013;46: 373-388.
- [11] Lin X. Numerical simulation of blast responses of ultra-high performance fibre reinforced concrete panels with strain-rate effect. *Construction and Building Materials*. 2018;176: 371-382.
- [12] Al-Salloum Y, Almusallam T, Ibrahim SM, Abbas H, Alsayed S. Rate dependent behavior and modeling of concrete based on SHPB experiments. *Cement and Concrete Composites*. 2015;55: 34-44.
- [13] Banerjee A, Dhar S, Acharyya S, Datta D, Nayak N. Determination of Johnson cook material and failure model constants and numerical modelling of Charpy impact test of armour steel. *Materials Science and Engineering: A*. 2015;640: 200-209.
- [14] Yang H, Yang X, Varma AH, Zhu Y. Strain-rate effect and constitutive models for Q550 high-strength structural steel. *Journal of Materials Engineering and Performance*. 2019;28: 6626-6637.
- [15] Mishra S, Meena H, Parashar V, Khetwal A, Chakraborty T, Matsagar V, Chandel P, Singh M. High strain rate response of rocks under dynamic loading using split Hopkinson pressure bar. *Geotechnical and Geological Engineering*. 2018;36: 531-549.
- [16] Malik A, Chakraborty T, Rao KS. Strain rate effect on the mechanical behavior of basalt: Observations from static and dynamic tests. *Thin-Walled Structures*. 2018;126: 127-137.
- [17] Zwiessler R, Kenkmann T, Poelchau MH, Nau S, Hess S. On the use of a split Hopkinson pressure bar in structural geology: High strain rate deformation of Seeberger sandstone and Carrara marble under uniaxial compression. *Journal of Structural Geology*. 2017;97: 225-236.
- [18] Thomas RJ, Sorensen AD. Review of strain rate effects for UHPC in tension. *Construction and Building Materials*. 2017;153: 846-856.
- [19] Yoo DY, Banthia N. Mechanical and structural behaviors of ultra-high-performance fiber-reinforced concrete subjected to impact and blast. *Construction and Building Materials*. 2017;149: 416-431.
- [20] Fakhimi A, Azhdari P, Kimberley J. Physical and numerical evaluation of rock strength in split Hopkinson pressure bar testing. *Computers and Geotechnics*. 2018;102: 1-11.
- [21] Abdelkarim OI, ElGawady MA. Performance of bridge piers under vehicle collision. *Engineering Structures*. 2017;140: 337-352.
- [22] Chen W, Hao H, Chen S. Numerical analysis of prestressed reinforced concrete beam subjected to blast loading. *Materials & Design*. 2015;65: 662-674.
- [23] Petrov YV, Morozov NF. On the modeling of fracture of brittle solids. *Journal of Applied Mechanics*. 1994;61(3): 710-712.
- [24] Petrov YV. Incubation time criterion and the pulsed strength of continua: Fracture, cavitation, and electrical breakdown. *Doklady Physics*. 2004;49(4): 246-249.
- [25] Petrov YV, Utkin AA. Dependence of the dynamic strength on loading rate. *Soviet Materials Science*. 1989;25: 153-156.

- [26] Petrov YV, Morozov NF, Smirnov VI. Structural macromechanics approach in dynamics of fracture. *Fatigue & Fracture of Engineering Materials & Structures*. 2003;26: 363-372.
- [27] Hibbeler RC. *Mechanics of Materials*. 10th ed. Pearson; 2017.
- [28] Anderson TL. *Fracture Mechanics: Fundamentals and Applications*. 4th ed. CRC Press; 2017.
- [29] Kolsky H. *Stress waves in solids*. New York: Dover Publications; 1963.
- [30] Lindholm US, Yeakley LM. High strain-rate testing: Tension and compression. *Experimental Mechanics*. 1968;8: 1-9.
- [31] Yokoyama T. Determination of dynamic fracture-initiation toughness using a novel impact bend test procedure. *Journal of Pressure Vessel Technology*. 1993;115: 389-397.
- [32] Zhang QB, Zhao J. A review of dynamic experimental techniques and mechanical behaviour of rock materials. *Rock Mechanics and Rock Engineering*. 2014;47: 1411-1478.
- [33] Xia K, Yao W. Dynamic rock tests using split Hopkinson (Kolsky) bar system – A review. *Journal of Rock Mechanics and Geotechnical Engineering*. 2015;7: 27-59.